Size-dependent momentum smearing effect of positron annihilation radiation in embedded nano Cu clusters

2008 J. Phys.: Condens. Matter 20 445203

(http://iopscience.iop.org/0953-8984/20/44/445203)

J. Phys.: Condens. Matter **20** (2008) 445203 (5pp) doi:10.1088/0953-8984/20/44/445203

Size-dependent momentum smearing effect of positron annihilation radiation in embedded nano Cu clusters

Z Tang[1], T Toyama[2], Y Nagai[2], K Inoue[2], Z Q Zhu[1] and M Hasegawa[2,3]

[1] Key Laboratory of Polar Materials and Devices (Ministry of Education of China), Department of Electronic Engineering, East China Normal University, Shanghai 200241, People's Republic of China
[2] The Oarai Center, Institute for Materials Research, Tohoku University, Ibaraki 311-1313, Japan
[3] Institute for Materials Research, Tohoku University, Sendai 980-8577, Japan

Received 18 April 2008, in final form 20 August 2008
Published 30 September 2008
Online at stacks.iop.org/JPhysCM/20/445203

Abstract
Momentum density distributions determined by the analysis of positron annihilation radiation in embedded nano Cu clusters in iron were studied by using a first-principles method. A momentum smearing effect originated from the positron localization in the embedded clusters is observed. The smearing effect is found to scale linearly with the cube root of the cluster's volume, indicating that the momentum density techniques of positron annihilation can be employed to explore the atomic-scaled microscopic structures of a variety of impurity aggregations in materials.

1. Introduction

Positron annihilation is a well-established technique to study vacancies and their aggregations in solids, because positrons can be sensitively trapped by the vacancy-type defects [1, 2]. Recently, it was found [3–10] that positrons can be trapped by non-vacancy-type nanoparticles embedded in a host material when the particles' positron affinities [2, 11–13] are higher than those of the host. The trapped positrons annihilate with the electrons of the nanoparticles and thus bring site-selective information on the microscopic and electronic structures of the particles through two emitted γ photons. By measuring the angular correlation distribution between two γ photons (angular correlation of annihilation radiation, ACAR) [1], the momentum density distributions of positron annihilation radiation in nanoparticles are then obtained.

A promising application of nanoparticle-trapped positrons is to study the microscopic and electronic structures of quantum dots embedded in semiconductors. A theoretical study by Saniz *et al* [14] predicted that, when an electron gas is confined by a spherical potential, its momentum density distribution will differ from the Fermi sphere of a free electron gas and the sharp difference between the electron occupations outside and inside the Fermi sphere will be smeared out. They found that the smearing effect scales linearly with the inverse of the radius of the confinement potential well (i.e. $\propto 1/r$). Weber *et al* [15] measured the momentum density distributions of the confined electrons in CdSe quantum dots by the positron coincidence Doppler broadening technique [16, 17]; a different scaling behavior ($\propto 1/r^2$) was observed and the discrepancy between the theoretical and experimental scaling indexes was attributed to the lattice effects of the quantum dots.

In this work, we tried to clarify the above issue by employing first-principles calculations of positron annihilation to a more realistic case of Cu precipitates in dilute FeCu alloys. Because the dilute FeCu alloys are the model alloys of the reactor pressure vessel (RPV) steels, the systems under study are of importance to the nuclear energy industry [18]. In particular, it has been known for a long time that the Cu precipitates play an important role in the embrittlement of the RPV steels [18, 19]. Therefore, identification and monitoring of nano Cu precipitates in the RPV steels are critical for safe operation of the nuclear reactors.

Previous works [3, 19, 20] have shown that positrons are indeed trapped by the Cu precipitates in the dilute FeCu alloys. However, in these alloy systems, both the Cu precipitates and the iron host are metallic so that neither electron confinement nor electron-confinement-induced Fermi surface smearing is

expected. Could the trapped positrons find applications in these metallic systems? We approach the issue here by calculating and analyzing the ACAR distributions of the trapped positrons in the bcc Cu clusters embedded in an iron matrix. We demonstrate that, due to the sampling effect of the trapped positrons, there is a size-dependent smearing of the momentum density distributions. The smearing effect is observed to scale linearly with $(1/\Omega)^{1/3}$, where Ω is the cluster's volume, indicating that the positron annihilation technique can be employed as a powerful tool to study the metallic quantum dots and precipitates in alloys.

2. Calculation

To simulate the embedded Cu clusters in iron, we generated coherent Cu clusters [28], Cu_6, Cu_{15}, Cu_{27} and Cu_{59}, in an 128-site supercell of bcc ferromagnetic Fe (figure 1). In the present work the experimental lattice parameter of bcc ferromagnetic iron, $a = 5.42a_0$ (a_0 is the Bohr radius) [29], is employed. The geometric and electronic structures of the simulated systems were optimized by using the iterative minimization technique [21, 22]. In the calculations, we employed a plane-wave basis set with a cutoff kinetic energy of 237.5 eV to expand the wavefunctions of the electrons and positron. The electron–ion and positron–ion interactions are represented by, respectively, the ultrasoft pseudopotential [23] and the full potential using the frozen core approximation. The electron–electron correlation was calculated within the generalized gradient approximation [24] and the positron–electron correlation effects (i.e. the correlation potential and the enhancement factor) were calculated based on the two-component density functional theory [11, 25] within the local density approximation (details about the method can be found in our previous publication [26]). In addition, we employed a $3 \times 3 \times 3$ Monkhorst–Pack type k-point mesh [27] to perform the first Brillouin zone (FBZ) integration in the calculation of the self-consistent electron charge density and ferromagnetism of iron was fully included in the present calculations. For the positron calculation (both the positron wavefunction and the positron charge density), only the Γ point is employed.

After the electron's and positron's wavefunctions are obtained, the 3D momentum density distribution of the positron–electron pair, $\rho(\mathbf{p})$, is calculated as

$$\rho(\mathbf{p}) = \sum_{i\mathbf{k}} f(\varepsilon_{i\mathbf{k}}) \left| \int \mathrm{e}^{-\mathrm{i}\mathbf{pr}} \psi_{+0}(\mathbf{r}) \psi_{i\mathbf{k}}(\mathbf{r}) \sqrt{g(\mathbf{r})} \mathrm{d}\mathbf{r} \right|^2 . \quad (1)$$

In the above equation, $\psi_{i\mathbf{k}}(\mathbf{r})$ is the wavefunction of the electron state with the band index i and the crystal momentum $\mathbf{k}$ ($\mathbf{k}$ is within the FBZ), f is its occupation number and $\mathbf{p} = \mathbf{k} + \mathbf{G}$ ($\mathbf{G}$ is the reciprocal lattice) is the momentum of the positron–electron pair associated with the crystal momentum $\mathbf{k}$. $\psi_{+0}(\mathbf{r})$ is the positron wavefunction at the Γ point and $g(\mathbf{r})$ is the enhancement factor describing the many-body effect of positron–electron correlation [11]. By projecting the calculated 3D momentum density distribution of the positron–electron pair $\rho(\mathbf{p})$ along a chosen axis p_z, the experimental two-dimensional angular correlation of positron annihilation radiation (2D-ACAR) spectrum can be simulated as $\rho(p_x, p_y) = \int \rho(\mathbf{p}) \mathrm{d}p_z$. For comparison, we also calculated the positron lifetime (τ), which is the inverse of the positron annihilation rate (λ) given by $\lambda = \pi r_0^2 c \int n_-(\mathbf{r}) n_+(\mathbf{r}) g(\mathbf{r}) \mathrm{d}\mathbf{r}$, where $n_-(\mathbf{r}) = \sum_{i\mathbf{k}} f(\varepsilon_{i\mathbf{k}}) |\psi_{i\mathbf{k}}(\mathbf{r})|^2$ is the electron density and $n_+(\mathbf{r}) = |\psi_{+0}(\mathbf{r})|^2$ is the positron density.

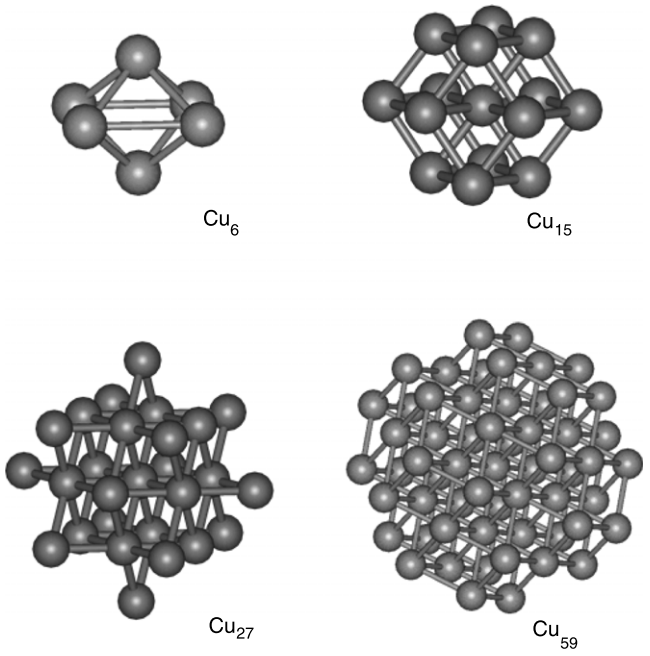

Figure 1. Structures of simulated Cu clusters embedded in the iron matrix.

3. Results and discussion

We start our discussions from the calculated positron states. The positron wavefunctions in the present calculations are found to be similar to our previous work [28, 30]. It is confirmed that even the smallest cluster in this work, Cu_6, can trap the positron, although there are considerable positron densities spilling out of the cluster, so that the positron has a certain probability to annihilate with the electrons of the iron matrix. However, since the positron annihilation lifetimes in bcc Cu (106 ps) and bcc Fe (104 ps) are very similar [28], the calculated lifetimes of the trapped positrons at the Cu clusters are nearly constant and are insensitive to details of the trapping centers.

However, the momentum density distributions of positron annihilation radiation are found to be very sensitive to the embedded Cu clusters. As an example, figure 2 presents the 2D projection of the calculated ACAR distributions (i.e. 2D-ACAR) along the [001] direction for the largest (Cu_{59}) and the smallest (Cu_6) clusters of this work, in comparison with that of bcc Cu bulk. Remarkable changes are observed when the positron annihilation site varies from the bcc Cu bulk to the Cu_6 cluster. For the bcc Cu bulk, the calculation shows that its Fermi surface is nearly spherical except for 12 necks connecting to the {110} Brillouin zone boundaries at the highly

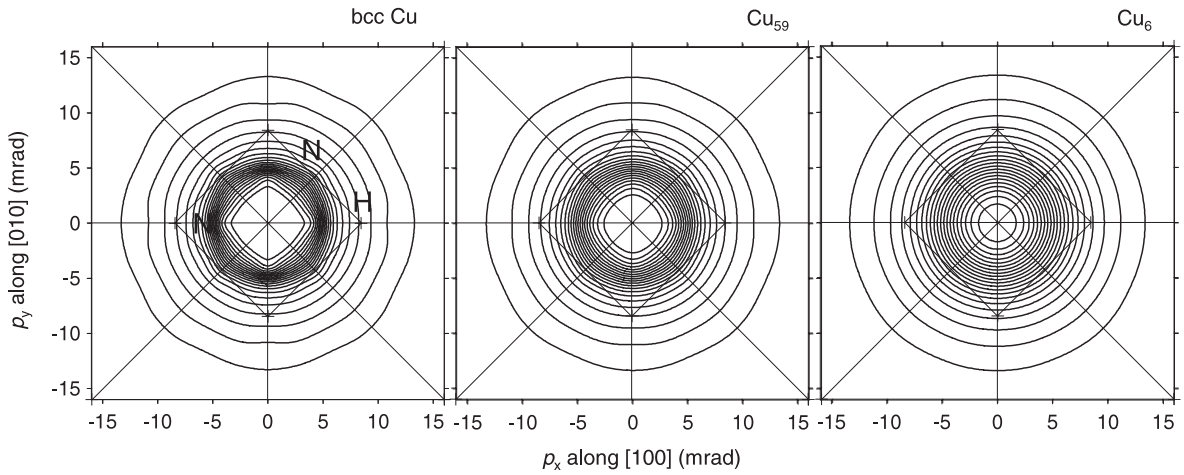

Figure 2. Contour plots of positron 2D-ACAR distributions projected along the [001] direction for bcc Cu bulk (left), embedded Cu_{59} cluster (middle) and embedded Cu_6 cluster (right). The contour-line interval is 1/21 of the maximum momentum density. Thin lines and characters denote the projections of the first Brillouin zone and the highly symmetric points, respectively.

symmetric N points. Therefore, the 2D-ACAR distribution of bcc Cu has higher momentum densities at the projections of N points [4, 28, 30] and drops rapidly outside the Fermi surface ($k_F \approx 5.18$ mrad) [28] (figure 2). These characteristic features are visible in the 2D-ACAR distribution for the Cu_{59} cluster but are gradually smeared out when the cluster size is further reduced to Cu_6.

The above 2D-ACAR distributions are contributed from the positron annihilations with both the electrons of Cu clusters and the electrons of the Fe matrix due to the positron density spilling out of the clusters. As the spilling positron density increases with reducing the size of the Cu cluster, the observed enhancement of the smearing effect may just represent a decrease of positron annihilation probability with the electrons of the Cu clusters. To clarify this issue, the ACAR contributions from the positron annihilations with the Fe matrix have to be subtracted.

Unfortunately, because the plane-wave basis set employed in the present calculations is non-local and is defined over the whole supercell, it is difficult to unambiguously decompose the positron annihilation rate. For this reason, we employed the superimposed atomic charge scheme proposed by Puska *et al* [31, 11], in which the positron annihilation rates with the electrons of Cu/Fe are explicitly

$$\lambda_{\mathrm{Cu/Fe}} = \pi r_0^2 c \int n_-^{\mathrm{Cu/Fe}}(\mathbf{r}) n_+(\mathbf{r}) g(\mathbf{r}) \mathrm{d}\mathbf{r}, \qquad (2)$$

where $n_-^{\mathrm{Cu/Fe}}(\mathbf{r}) = \sum_I \rho_{\mathrm{at}}^{\mathrm{Cu/Fe}}(\mathbf{r} - \mathbf{R}_I)$ is the superimposition of the atomic charge ($\rho_{\mathrm{at}}^{\mathrm{Cu/Fe}}$) specific to Cu or Fe, and the enhancement factor $g(\mathbf{r})$ depends on the total charge [$= n_-^{\mathrm{Cu}}(\mathbf{r}) + n_-^{\mathrm{Fe}}(\mathbf{r})$]. The positron lifetimes calculated as the inverse of the total annihilation rate [$\tau = 1/(\lambda_{\mathrm{Cu}} + \lambda_{\mathrm{Fe}})$] based on this scheme differ only slightly from those based on the plane-wave scheme (by less than 1 ps). The fraction of spilling positron annihilation with the Fe electrons is then determined as $f_{\mathrm{Fe}} = \lambda_{\mathrm{Fe}}/(\lambda_{\mathrm{Cu}} + \lambda_{\mathrm{Fe}})$ and its contribution to the positron 2D-ACAR, $f_{\mathrm{Fe}}\rho_{\mathrm{Fe}}(\mathbf{p})$, is subtracted from the calculated total

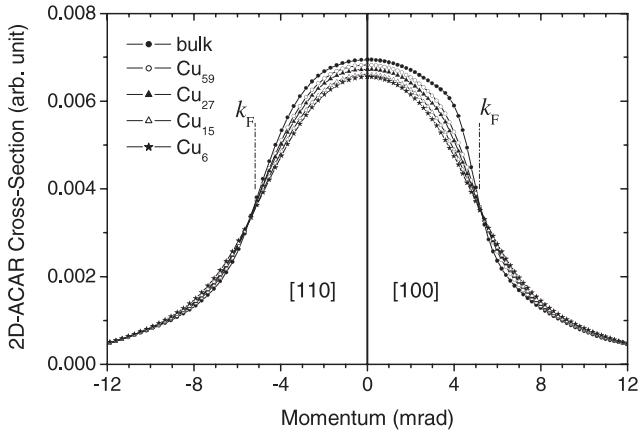

Figure 3. Cross sections of normalized 2D-ACAR distributions for the embedded Cu clusters after the spilling positron annihilations in the Fe matrix are subtracted.

2D-ACAR (here $\rho_{\mathrm{Fe}}(\mathbf{p})$ is the calculated 2D-ACAR for bcc ferromagnetic Fe bulk and we assume that the momentum distribution of the spilling positron annihilation with the Fe electrons is similar to that of bcc ferromagnetic Fe bulk).

Figure 3 presents the decomposed 2D-ACAR cross sections along the [100] and [110] directions after the Fe contribution is subtracted. From figure 3, we see clearly that there indeed is a momentum smearing effect around k_F and the effect is enhanced with reducing the Cu cluster size. Since both the Cu clusters and the Fe matrix are metallic, there is no confined electron in the present alloys and the observed momentum smearing effect cannot be attributed to the electron confinement; instead, it is originated from the trapped positron sampling the local electronic structures of the Cu clusters, somewhat similar to the effect of a confined positron in free volumes discussed by Calloni *et al* [32]. It can be understood that, when the positron annihilation site changes from the bcc Cu bulk to the Cu_6 cluster, the positron-sampled momentum density distribution is subjected to a variation from crystal-like

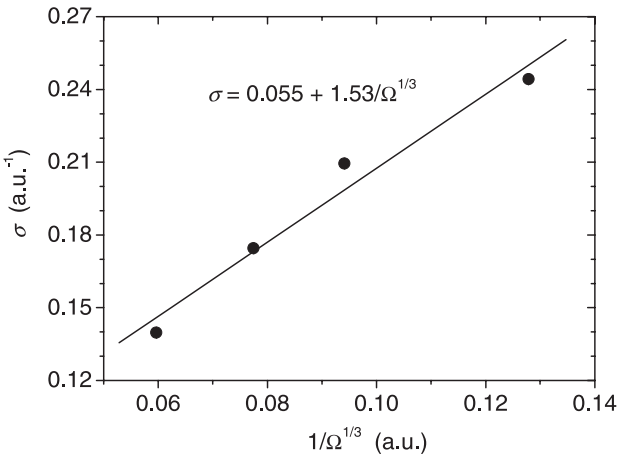

Figure 4. Momentum smearing parameter (σ) versus the cube root of Cu cluster's volume ($\Omega^{1/3}$). The error bars of the momentum smearing parameters are smaller than their point size.

to atom-like, namely, the rapid drop of the momentum density around k_F observed in the bulk will be smeared out, as shown in figure 3.

To quantitatively describe the above momentum smearing effect, we tried to reconstruct the decomposed 2D-ACAR for the Cu clusters [$\rho(\mathbf{p})$] by convoluting the 2D-ACAR for the bulk [$\rho_{Cu}(\mathbf{p})$] with a 2D circular Gaussian function $g(\mathbf{p}) = (1/2\pi\sigma^2)e^{-p^2/2\sigma^2}$ and employed σ as the momentum smearing parameter to characterize the effect. The best fit to σ is then determined by minimizing the object function

$$\phi(\sigma) = \int \left| \rho(\mathbf{p}) - \int g(\mathbf{p}-\mathbf{q})\rho_{Cu}(\mathbf{q})d\mathbf{q} \right|^2 d\mathbf{p}, \qquad (3)$$

within the momentum region of $p \leqslant 24$ mrad and the obtained σ's are 1.020±0.007, 1.265±0.008, 1.525±0.007 and 1.780±0.005 mrad, for Cu_6, Cu_{15}, Cu_{27}, and Cu_{59}, respectively.

Next, we verify if the calculated momentum smearing has some scaling behavior with the cluster size. As the shapes of the smaller clusters (Cu_6 and Cu_{15}) differ considerably from a sphere, we here choose the volume Ω ($=N_{Cu}\upsilon_{Cu}$, $\upsilon_{Cu} = a^3/2$ is the average volume of a Cu atom in the Fe matrix) instead of the radius to characterize the cluster. It is observed that there is a good linear correlation between σ and $\Omega^{1/3}$, i.e. $\sigma = 0.055 + 1.53/\Omega^{1/3}$ (in atomic unit a_0^{-1} (=7.297 mrad)) (figure 4), indicating that the momentum smearing effect scales linearly with the cube root of the Cu cluster's volume. This result is consistent with the theory of Saniz *et al* [14], although the smearing effect discussed here is of a different but more general origination, i.e. by the trapped positrons sampling the local electronic structure of the embedded cluster. Therefore, the present work demonstrates that the momentum distributions in the nano particles sampled by positrons can be employed to study the microstructures of a variety of impurity aggregations in materials.

Finally, it is noteworthy that the scaling relationship obtained here cannot be extrapolated to the very large clusters as $\Omega \to \infty$, $\sigma \nrightarrow 0$ (equation (3)). The comparisons between the reconstructed 2D-ACAR distributions and the decomposed ones for the embedded Cu clusters in bcc ferromagnetic Fe indicate that these computational errors are less than 5%. The results presented in figure 4 show that the good linear scaling relationship (equation (3)) is valid at least up to the cluster size of 27 atoms.

Acknowledgments

This work is partly supported by the Grant-in-Aid for Scientific Research of the Ministry of Education, Science and Culture, Japan (nos. 17002009, 18686077 and 15106015) and the Radioactive Waste Management Funding. One of the authors (ZT) is supported by the State Key Basic Research Program of China (no. 2007CB924902), the National Science Foundation of China (no. 10775053), The Program of New Century Excellent Talents in University, Ministry of Education of China, and the Shanghai Pujiang Program (no. 08PJ140450).

References

[1] Dupasquier A and Mills A P Jr (ed) 1995 *Positron Spectroscopy of Solids* (Amsterdam: IOS Press)
[2] Krause-Rehberg R and Leipner H S 1999 *Positron Annihilation in Semiconductors* (Berlin: Springer)
[3] Nagai Y, Hasegawa M, Tang Z, Hempel A, Yubuta K, Shimamura T, Kawazoe Y, Kawai A and Kano F 2000 *Phys. Rev.* B **61** 6574
[4] Nagai Y, Chiba T, Tang Z, Akahane T, Kanai T, Hasegawa M, Takenaka M and Kuramoto E 2001 *Phys. Rev. Lett.* **87** 176402
[5] Xu J, Mills A P Jr, Ueda A, Henderson D O, Suzuki R and Ishibashi S 1999 *Phys. Rev. Lett.* **83** 4586
[6] van Huis M A, van Veen A, Schut H, Kooi B J and De Hosson J Th 2003 *Phys. Rev.* B **67** 235409
[7] Druzhkov A P, Perminov D A, Arbuzov V L, Stepanova N N and Pechorkina N L 2004 *J. Phys.: Condens. Matter* **16** 6395
[8] Cizek J, Melikhova O, Prochazka I, Kuriplach J, Stulikova I, Vostry P and Faltus J 2005 *Phys. Rev.* B **71** 064106
[9] Makkonen I, Hakala M and Puska M J 2006 *Phys. Rev.* B **73** 035103
[10] Eijt S W H, van Veen A, Schut H, Mijnarends P E, Denison A B, Barbiellini B and Bansil A 2006 *Nat. Matter* **5** 23
[11] Puska M J and Nieminen R M 1994 *Rev. Mod. Phys.* **66** 841
[12] Brauer G, Puska M J, Sob M and Korhonen T 1995 *Nucl. Eng. Design* **158** 149
[13] Kuriplach J, Sob M, Brauer G, Anwand W, Nicht E-M, Coleman P G and Wagner N 1999 *Phys. Rev.* B **59** 1948
[14] Saniz R, Barbiellini B and Denison A 2002 *Phys. Rev.* B **65** 245310
[15] Weber M H, Lynn K G, Barbiellini B, Sterne P A and Denison A B 2002 *Phys. Rev.* B **66** 041305(R)
[16] Lynn K G, MacDonald J R, Boie R A, Feldman L C, Gabbe J D, Robbins M F, Bonderup E and Golovchenko J 1977 *Phys. Rev. Lett.* **38** 241
[17] Asoka-Kumar P, Alatalo M, Ghosh V J, Kruseman A C, Nielsen B and Lynn K G 1996 *Phys. Rev. Lett.* **77** 2097
[18] Glade S C, Wirth B D, Asoka-Kumar P, Sterne P A and Odette G R 2004 *Mater. Sci. Forum* **445/446** 87
[19] Asoka-Kumar P, Wirth B D, Sterne P A and Odette G D 2002 *Phil. Mag. Lett.* **82** 609

[20] Nadesalingam M, Kim S, Fazleev N G, Fry J L, Nagai Y, Hasegawa M and Weiss A H 2004 *Mater. Sci. Forum* **445/446** 156
[21] Car R and Parrinello M 1985 *Phys. Rev. Lett.* **55** 2471
[22] Payne M C, Teter M P, Allen D C, Arias T A and Joannopoulos J D 1992 *Rev. Mod. Phys.* **64** 1045
[23] Kresse G and Hafner J 1994 *J. Phys.: Condens. Matter* **6** 8245
[24] Perdew J P and Wang Y 1992 *Phys. Rev.* B **45** 13244
[25] Puska M J, Seitsonen A P and Nieminen R M 1995 *Phys. Rev.* B **52** 10947
[26] Tang Z, Hasegawa M, Chiba T, Saito M, Sumiya H, Kawazoe Y and Yamaguchi S 1998 *Phys. Rev.* B **57** 12219
[27] Monkhorst H J and Pack J D 1976 *Phys. Rev.* B **13** 5188
[28] Tang Z, Hasegawa M, Nagai Y and Saito M 2002 *Phys. Rev.* B **65** 195108
[29] Kittle C 1996 *Introduction to Solid State Physics* 7th edn (New York: Wiley) p 23
[30] Hasegawa M, Tang Z, Nagai Y, Chiba T, Kuramoto E and Takenaka M 2005 *Phil. Mag.* **85** 467
[31] Puska M J and Nieminen R M 1983 *J. Phys. F: Met. Phys.* **13** 333
[32] Calloni A, Dupasquier A, Ferragut R, Folegati P, Iglesias M M, Makkonen I and Puska M J 2005 *Phys. Rev.* B **72** 054112